Emulsification of Partially Miscible Liquids Using Colloidal Particles: Nonspherical and Extended Domain Structures

Paul S. Clegg,*[,†,‡] Eva M. Herzig,[†,‡] Andrew B. Schofield,[†] Stefan U. Egelhaaf,[§] Tommy S. Horozov,[||] Bernard P. Binks,[||] Michael E. Cates,[†] and Wilson C. K. Poon[†,‡]

SUPA, School of Physics, University of Edinburgh, Edinburgh, EH9 3JZ, United Kingdom, Collaborative Optical Spectroscopy, Micromanipulation and Imaging Centre (COSMIC), University of Edinburgh, Edinburgh, EH9 3JZ, United Kingdom, Institut für Physik der kondensierten Materie, Heinrich-Heine-Universität, Universitätstrasse 1, D-40225 Düsseldorf, Germany, and Surfactant & Colloid Group, Department of Chemistry, University of Hull, Hull, HU6 7RX, United Kingdom

Received December 21, 2006. In Final Form: March 6, 2007

We present microscopy studies of particle-stabilized emulsions with unconventional morphologies. The emulsions comprise pairs of partially miscible fluids and are stabilized by colloids. Alcohol−oil mixtures are employed; silica colloids are chemically modified so that they have partial wettability. We create our morphologies by two distinct routes: starting with a conventional colloid-stabilized emulsion or starting in the single-fluid phase with the colloids dispersed. In the first case temperature cycling leads to the creation of extended fluid domains built around some of the initial fluid droplets. In the second case quenching into the demixed region leads to the formation of domains which reflect the demixing kinetics. The structures are stable due to a jammed, semisolid, multilayer of colloids on the liquid−liquid interface. The differing morphologies reflect the roles in formation of the arrested state of heterogeneous and homogeneous nucleation and spinodal decomposition. The latter results in metastable, bicontinuous emulsions with frozen interfaces, at least for the thin-slab samples, investigated here.

1. Introduction

Arrested phase separation is a productive route for creating metastable materials with potentially useful properties. For example, the texture and hardness of some metallic alloys is the result of a metastable inhomogeneous organization.[1,2] An initially homogeneous solid solution will begin to separate on cooling into the demixed regime. Rearrangements occur, often mediated by vacancies. Changes become immeasurably slow due to the low mobility of the two constituents. The final structure and its properties reflect the annealing schedule used. In an analogous way, the mixed phase of some pairs of liquids will also phase separate in response to changes in temperature or pressure.[3] However, here the analogy breaks down: with liquids the domain boundaries will not arrest until the phases have fully separated due to their high mobility. Creating static fluid domains with a large stable interface would be intriguing and potentially useful. To this end, we explored how domain boundaries in phase-separating fluids can be locked in place using colloidal particles and also how such pinned domains respond to thermal cycling. Our results show arrested microstructures in liquids.

The morphology of microstructures formed as a result of liquid−liquid demixing strongly depends on the transition kinetics.[2] These are controlled by the pathway into the demixed region.[4] Shallow or slow quenches will lead to phase separation via homogeneous nucleation: droplets form (larger than a critical size) that coarsen over time until macroscopic domains are created. Such droplets are always preferred when the volume fractions of the two constituents are highly mismatched. Deep or fast quenching leads, in contrast, to spinodal decomposition: a large-scale instability that can occur when the domains have almost equal volume fractions. Instead of droplets, convoluted bicontinuous domains form. The domains are characterized by a single dominant length scale with a time dependence that reflects different coarsening mechanisms. Mean-field theory divides the kinetics of phase separation into these two distinct cases.[5] It is suggested, following a more complete analysis, that there is an intermediate regime characterized by formation of ramified nuclei.[6]

To arrest microstructures in demixing fluid systems we must raise the energy cost of domain coarsening. To do this we need to introduce a third component into our liquid mixtures. Our approach is to make use of the surfactant-like properties of colloidal particles. These sequester to liquid−liquid interfaces if they have partial wettability.[7] The colloid reduces the area of shared interface between the liquids, giving rise to an energy barrier. The change in interfacial energy, ΔG_{int}, varies with the liquid−liquid/colloid wetting angle, θ_{w}, according to

$$\Delta G_{\mathrm{int}} = \pi r^2 \gamma [1 \pm \cos(\theta_{\mathrm{w}})]^2 \qquad (1)$$

where r is the colloid radius and γ is the interfacial tension. This change is often more than sufficient to ensure that the colloid is irreversibly trapped (e.g., $\Delta G_{\mathrm{int}} \approx 10^4\ k_{\mathrm{B}}T$ for $r = 0.25\ \mu$m neutrally wetting colloids on an interface with $\gamma \approx 1$ mN m^{-1}). The behavior is somewhat analogous to that of amphiphilic surfactants. Important differences are that the surface of the colloids is isotropic and that the energy barrier holding the colloid

[†] School of Physics, University of Edinburgh.
[‡] COSMIC, University of Edinburgh.
[§] Heinrich-Heine-Universität.
[||] University of Hull.

(1) Martin, J. W. *Precipitation Hardening*, 2nd ed.; Butterworth-Heinemann: Oxford, 1998.
(2) Ma, E. *Prog. Mater. Sci.* **2005**, *50*, 413.
(3) Rowlinson, J. S.; Swinton, F. L. *Liquids and Liquid Mixtures*, 3rd ed.; Butterworths: London, 1982.
(4) Debenedetti, P. G. *Metastable liquids: concepts and principles*; Princeton University Press: New Jersey, 1996.
(5) Onuki, A. *Phase Transition Dynamics*; Cambridge University Press: Cambridge, 2002.
(6) Unger, C.; Klein, W. *Phys. Rev. B* **1984**, *29*, 2698.
(7) *Colloidal Particles at Liquid Interfaces*; Binks, B. P., Horozov, T. S., Eds.; Cambridge University Press: Cambridge, 2006; pp 1−74.

10.1021/la063707t CCC: $37.00
Published on Web 04/18/2007

to the interface is usually many orders of magnitude larger (see Appendix). The first difference may make colloids less effective at stabilizing interfaces, while the second suggests they will be far superior. Another difference is that while amphiphiles find it favorable to create a fluid−fluid interface on which to reside, colloids (of homogeneous surface chemistry) generally do not. The free energy of a colloidal system is minimized when the surface area of the liquid phases is as low as possible: coating the surface with colloids reduces its area further. Structures of large interfacial area, like those discussed here, are generally metastable.[7]

Extensive studies have now been carried out on the formation and properties of colloid-stabilized emulsions.[7−10] These have focused on colloid-stabilized *droplets* of immiscible fluids. Such droplets will coarsen until the colloids are close enough to form a protective barrier; for hard-sphere colloids this occurs when the particles are jammed together. Our studies of microstructure can be viewed as an extension of this research to the cases of nonspherical and extended fluid domains in partially miscible fluids. Deformed particle-coated interfaces have also been created by direct manipulation of air bubbles[11,12] and liquid jets.[13]

Studies of the interaction of dispersed particles with a newly created interface during liquid−liquid demixing were initiated almost 100 years ago[14,15] The proclivity of particles to sequester to the interface was found to depend on the depth of cooling below the critical point due to the increase in the interfacial tension. More recently, Gallagher and Maher explored the reversible aggregation of particles during phase separation.[16] They also found a strong dependence of the behavior on the magnitude of the temperature change. For some quench routes they observed formation of metastable structures. These were not studied in any detail; it is possible that they were similar to some of the liquid−liquid microstructures we examine here. Very recent studies examined the behavior of silica nanoparticles in phase-separating polymers.[17] The system chosen has a lower critical point, and one series of particles used is partially wetted by both polymers. For thin films, arrested structures are observed to form following slow quenching and a coarsening period lasting many hours. These structures may also be analogous to some of those reported here for binary liquids. Two major differences, compared to our studies of simple liquids with colloids, are that[17] the time scales involved are very long and the sample thickness employed is very thin compared to the typical domain size.

To understand the colloidal stabilization of interfaces we need to pay close attention to wetting, heterogeneous nucleation, interfacial curvature, and interfacial tension. We outline the role of each in turn. Colloid stabilization creates additional complexity due to induced changes to the underlying liquid−liquid phase behavior and the appearance of new kinetic pathways. The principal effects are pretransitional wetting and heterogeneous nucleation. Beysens and Esteve systematically investigated the pretransitional wetting of colloidal particles approaching binary−fluid phase separation,[18] where one of the fluids is likely to preferentially wet the colloid surface. Close to the transition this fluid will form a wetting layer around the particles. This can lead to particle aggregation and sedimentation, the latter rendering the particles unavailable to pin the liquid−liquid domain boundaries. The presence of colloids will also favor heterogeneous nucleation on quenching into the demixed regime. The rate of heterogeneous nucleation, J_{het}, relative to the rate of homogeneous nucleation, J_{hom}, depends on wetting angle according to[4]

$$\frac{J_{het}}{J_{hom}} = \frac{a}{N_{tot}^{1/3}} \exp\left\{\frac{W_{min}}{k_B T}\left(1 - \frac{(1 - \cos\theta_w)^2(2 + \cos\theta_w)}{4}\right)\right\} \quad (2)$$

Here, a is the surface available for heterogeneous nucleation per unit bulk volume of liquid phase, W_{min} is the minimum work required to form a nucleus at the solid surface, and N_{tot} is the number density of the majority phase. Thus, neutral wetting ($\theta_w \approx 90°$) suppresses the rate of heterogeneous nucleation compared to the case of complete wetting by the minority phase ($\theta_w = 0°$). The argument of the exponential in eq 2 falls by half in this case, so for $W_{min} > k_B T$ the degree of suppression can be substantial. It has been suggested by Tanaka that heterogeneous nucleation is more extreme for quenched binary-liquid mixtures of nearly equal volume fractions.[19] This is the case where coarsening can occur via hydrodynamic flow along bicontinuous tubes. The hydrodynamic flow of fluid along the tubes leads to enhanced formation of a wetting layer. This effect becomes dominant when quenching a demixing fluid close to flat surfaces.

In order to arrest nonspherical liquid domains using an interfacial layer of colloids it is necessary to accommodate variations in the mean curvature of the liquid−liquid interfaces on a length scale that is large compared to that of the colloids. Studies by Binks and co-workers[20] have shown that the phase which preferentially wets the particles is most likely to form the continuous phase. Hence, a particular surface chemistry will tend to favor one sign of curvature for the liquid−liquid interface. To accommodate variations it is essential that the colloids should exhibit similar wetting characteristics with respect to both fluid phases, which demands careful tuning of the surface chemistry. This criterion is necessary but not sufficient. Constancy of the Laplace pressure across a fluid interface in equilibrium means that if variations in mean curvature are present on the macroscale, the interface either is solid or has effectively zero interfacial tension (see also the Appendix). The former appears more likely for an interfacially jammed layer of colloids; imperfections in the arrangements of the colloids at the interface were observed to be static, supporting the idea of a solid interfacial layer. Zero tension should instead impart large temporal variations in mean curvature, which we do not observe. Furthermore, in a preliminary account of some of our studies[21] we also demonstrated that on warming a colloid-stabilized emulsion toward the single-fluid phase the interface can undergo a buckling instability. This suggests reduction of interfacial tension from a high value and is similar to the behavior of two-dimensional colloidal crystals at flat interfaces,[22,23] again suggesting the presence of a solid

(8) Yeung, A.; Dabros, T.; Czarnecki, J.; Masliyah, J. *Proc. R. Soc. London A* **1999**, *455*, 3709.
(9) Stancik, E. J.; Fuller, G. G. *Langmuir* **2004**, *20*, 4805.
(10) Horozov, T. S.; Binks, B. P. *Angew. Chem., Int. Ed.* **2006**, *45*, 773.
(11) Subramaniam, A. B.; Abkarian, M.; Mahadevan, L.; Stone, H. A. *Nature* **2005**, *438*, 930.
(12) Subramaniam, A. B.; Abkarian, M.; Mahadevan, L.; Stone, H. A. *Langmuir* **2006**, *22*, 10204.
(13) Edmond, K. V.; Schofield, A. B.; Marquez, M.; Rothstein, J. P.; Dinsmore, A. D. *Langmuir* **2006**, *22*, 9052.
(14) Winkelblech, K. *Z. Angew. Chem.* **1908**, *19*, 1953.
(15) Lash Miller, W.; McPherson, R. H. *J. Phys. Chem.* **1908**, *12*, 706.
(16) Gallagher, P. D.; Maher, J. V. *Phys. Rev. A* **1992**, *46*, 2012.
(17) Chung, H.-J.; Ohno, K.; Fukuda, T.; Composto, R. J. *Nano Lett.* **2005**, *5*, 1878.
(18) Beysens, D.; Esteve, D. *Phys. Rev. Lett.* **1985**, *54*, 2123.
(19) Tanaka, H. *Phys. Rev. E* **1996**, *54*, 1709.
(20) Binks, B. P. *Curr. Opin. Colloid Interface Sci.* **2002**, *7*, 21.
(21) Clegg, P. S.; Herzig, E. M.; Schofield, A. B.; Horozov, T. S.; Binks, B. P.; Poon, W. C. K.; Cates, M. E. *J. Phys.: Condens. Matter* **2005**, *17*, S3433.
(22) Aveyard, R.; Clint, J. H.; Nees, D.; Quirke, N. *Langmuir* **2000**, *16*, 8820.
(23) Vella, D.; Aussillous, P.; Mahadevan, L. *Europhys. Lett.* **2004**, *68*, 212.

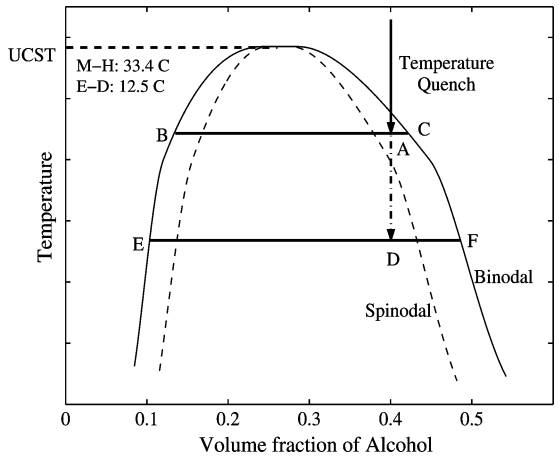

Figure 1. Generic alcohol−oil phase diagram showing binodal (solid line) and spinodal (dashed line). Liquids are miscible above the upper critical solution temperature (UCST). A sample quenched to A will nucleate droplets with composition B coexisting with a continuous background of composition C. A sample quenched to D will separate into domains of compositions E and F via spinodal decomposition.

layer. With our protocols, the interfacial layer is several particles thick;[21] similar multilayers have been observed using ellipsometry.[24]

In this paper we will show how fluid domain structures can be pinned by colloidal particles using two different routes to creating extended nonspherical domains. In section 2 we describe the materials used and the surface chemistry procedures required and summarize the different quenching approaches. In section 3 we begin by presenting results for the different protocols for creating new domains and discuss how they relate to the underlying phase behavior; the limit on the thickness of the sample will be discussed. We will then explore the behavior of colloid-stabilized droplets on warming toward miscibility. Finally, in section 4 we compare our results to recent computer simulations, draw conclusions, and look toward other possible quench routes. The Appendix describes the complex variation in the macroscopic interfacial tension due to the colloids.

2. Experimental Techniques

2.1. Materials. The liquids methanol (Aldrich, >99.9%), ethanol (Fisher, 99.8%), hexane (Fluka, ≥99.5%), and dodecane (Aldrich, >98%) were used as received. The relevant binary combinations are methanol−hexane (with an upper critical solution temperature (UCST) of 33.4 °C for 27.5:72.5 alcohol:oil by volume[25]) and ethanol−dodecane (with an UCST of 12.5 °C for 36.1:63.9 alcohol:oil[26]). A generic alcohol−oil phase diagram is shown in Figure 1. The composition used in many of these experiments was off-critical (marked by arrow in Figure 1); it was chosen to be half way between critical and equal volumes. The silica colloids were synthesized using the Stöber procedure[27] ($r = 220 \pm 7$ nm). For our studies it was required that the silica surface should have partial wettability with the alcohol and oil. The surface chemistry was modified using a silanization procedure previously described.[28] The concentration of the silanizing agent, dichlorodimethylsilane (DCDMS; Fluka, ≥99.5%), was varied to give batches of particles with a range of wetting properties. For each pair of liquids the ideal surface chemistry was chosen by testing which batch of particles would stabilize a macroscopic droplet emulsion for the longest. This technique only demonstrates the optimal surface chemistry for a particular temperature. Variation with temperature is anticipated as the composition of the phase-separated fluids varies continuously. At extremely low temperatures, where the two fluids are close to being pure alcohol and pure oil, the same batch of colloids will definitely not have similar wetting properties with respect to the two phases.

Silica particles with surface chemistries in the range of interest disperse easily in pure methanol. By contrast, these particles aggregate quite quickly in pure hexane. This may be due to capillary wetting: the silica particles experience induced attractive interactions due to polar impurities in the oil.[29]

2.2. Preparation. The sample cells for most of our experiments were capillaries $0.2 \times 4.0 \times 50.0$ mm^3 (VitroCom). The borosilicate walls are 0.2 mm thick. Where specifically mentioned, $0.4 \times 8.0 \times 50.0$ mm^3 capillaries were employed to yield a larger sample volume (walls 0.4 mm thick). Experiments involving slow warming and cooling were carried out under the microscope using a temperature stage (Linkam Scientific Instruments). Prior to quenching dispersed particle samples, the liquids were combined in an incubator (typically at 45 °C for methanol−hexane and 28 °C for ethanol−dodecane). The colloids (1−2% by volume) were dispersed using an ultrasound processor (Sonics and Materials) operating at 20 kHz for 2 min at 2−3 W power. The temperature was kept well above the binodal in order to avoid the wetting/aggregation regime discovered in ref 18. Where required, samples were cooled by quenching in a cryogen bath.

As detailed below, both the starting condition of the samples and the cooling technique determined the structures formed. We used a range of techniques to cool our samples quickly.[30,31] In order to elucidate the link between structure and route it is essential to determine the relative cooling rates. To this end we measured the cooling rates in our experimental geometry. A type-K thermocouple (Omega) was mounted within a sample cell, and the cooling rate was recorded via an acquisition card (National Instruments) during quenching. A comparison of the cooling rates for submersion in an ice bath, a bath of solid CO_2 in hexane, and finally a liquid nitrogen bath are shown in Figure 2. The curves have a simple form for ice and dry ice with the latter yielding a quicker and deeper quench. The cooling curve for liquid nitrogen begins with a more gentle slope, while the cryogen is induced to boil close to the sample holder. Once the boiling ceases the cooling rate becomes much more rapid. The initial rate is slower than that of dry ice and comparable to ice. The inset to Figure 2 is a comparison of the cooling rates using liquid nitrogen for the two different thicknesses of sample holder.

2.3. Characterization. We studied our emulsions using microscopy techniques. These included bright-field and phase-contrast microscopy using an Olympus BX50 microscope. Characterization as a function of depth was carried out using laser confocal microscopy. Nikon TE300 and TE800 microscopes with a BioRad Radiance 2100 scanner operating an Ar-ion laser were employed for this purpose. No fluorescent dyes were used in these studies. The contrast in refractive index between the silica and the liquids was sufficient to provide clear images up to at least 100 μm into the sample. Stacks of images were rendered using the ImageJ software package.[32]

3. Results and Discussion

We first examine emulsion formation starting from dispersed particles in the mixed phase (section 3.1). We go on to describe (section 3.2) our studies of particle-stabilized emulsion droplets being warmed out of the demixed region. Finally, we look at this system when it is warmed and then recooled in various ways

(24) Binks, B. P.; Clint, J. H.; Dyab, A. K. F.; Fletcher, P. D. I.; Kirkland, M.; Whitby, C. P. *Langmuir* **2003**, *19*, 8888.
(25) Hradetzky, G.; Lempe, D. A. *Fluid Phase Equilib.* **1991**, *69*, 285.
(26) Dürr, U.; Mirzaev, S. Z.; Kaatze, U. *J. Phys. Chem. A* **2000**, *104*, 8855.
(27) Stöber, W.; Fink, A.; Bohm, E. *J. Colloid Interface Sci.* **1968**, *26*, 62.
(28) Horozov, T. S.; Aveyard, R.; Clint, J. H.; Binks, B. P. *Langmuir* **2003**, *19*, 2822.
(29) Israelachvili, J. N. *Intermolecular and Surface Forces*, 2nd ed.; Academic Press: San Diego, 1992.
(30) Walker, L. J.; Moreno, P. O.; Hope, H. *J. Appl. Crystallogr.* **1998**, *31*, 954.
(31) Kriminski, S.; Kazmierczak, M.; Thorne, R. E. *Acta Crystallogr., Sect. D* **2003**, *59*, 697.
(32) Rasband, W. S. *ImageJ*; U.S. National Institute of Health: Bethesda, MD, 1997−2006; http://rsb.info.nih.gov/ij/.

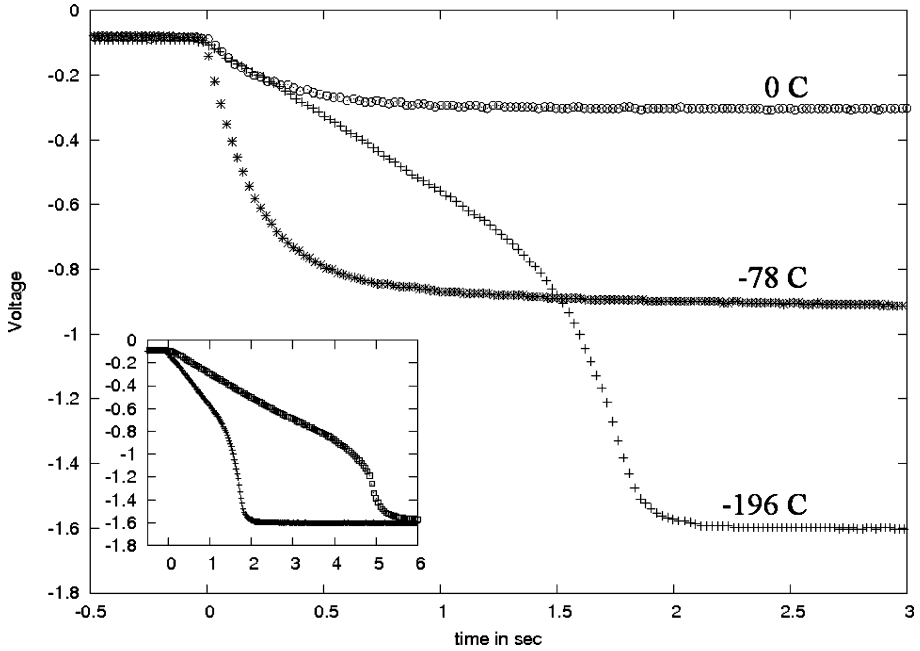

Figure 2. Sample cooling characteristics measured using a thermocouple embedded in a 200 μm deep sample cell. The different cooling techniques are submerging in an ice bath (open circles), a liquid nitrogen bath (crosses), and a bath of hexane containing solid CO_2 (asterisks). (Inset) Comparison of the rate of cooling using liquid nitrogen for 200 and 400 μm deep (open squares) cells.

(section 3.3). In all cases we interpret our results to elucidate the dominant mechanisms controlling the formation and properties of the emulsions.

3.1. Phase Separation in the Presence of Dispersed Particles. Our route to creation of novel emulsions begins with dispersed particles in the mixed phase. The system starts without any liquid−liquid interfaces for particle trapping. Below we present results for different cooling protocols. The variations in structure with protocol are shown in cartoon form in Figure 3. For slow, shallow cooling a particle-stabilized droplet emulsion is created with largely spherical droplets (Figure 4). This is the starting point for our studies in sections 3.2 and 3.3. It appears that the mixed fluid is separating via nucleation and growth. Hence, liquid−liquid interface appears and particles are trapped on it. As the droplets coarsen the interfacial area decreases until the particle layer becomes more densely packed. Eventually the particles are in close contact on the interface and the system jams (Figure 4).

Figures 5 and 6 show the structures formed instead by the fast, deep cooling of samples containing dispersed particles. The structures in Figure 5 were created by immersing the sample in a dry ice bath. This yields faster cooling than with ice (see Figure 2). Phase-contrast microscopy was employed for Figure 5a,b; the structures are wholly unlike the droplets observed before (Figure 4). Instead, the structure includes substantial regions of flat interface and some tube-like areas. Not all tubes were permanently stable, as can be seen from the frozen-in *pinch off relics* in Figure 5a,b). For this preparation route, the particle-laden interface was insufficient to suppress the Rayleigh−Plateau instability. Figure 6 shows confocal microscopy images (rendered using the ImageJ software package[32]) of bicontinuous structures created by deep quenching of a methanol−hexane mixture doped with colloidal silica particles. The liquid composition is the same as that for Figure 5, while here a higher volume fraction of particles was used (2% rather than 1.3%). The sample shown in Figure 6a was obtained by first dipping it in liquid nitrogen for 5 s and then cooling it in a CO_2 bath (−78 °C) for 5 min. The sample shown in Figure 6b was obtained by cooling it in liquid nitrogen for 30 s before submerging it in the CO_2 bath. The small differences in fabrication procedure appear to be reflected in a

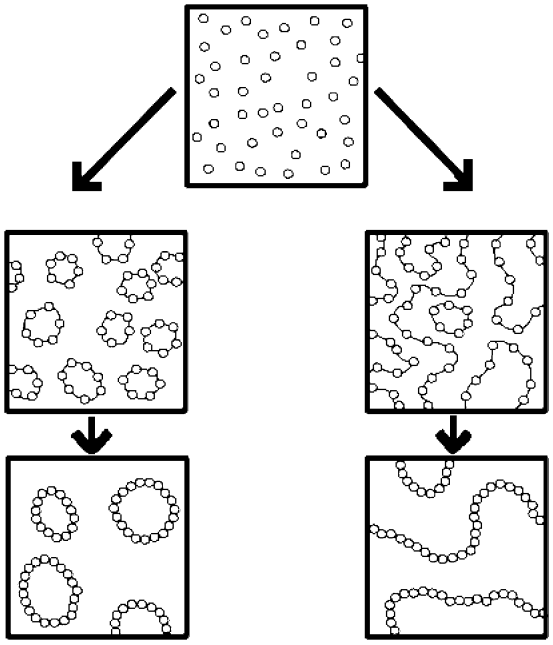

Figure 3. Cartoon illustrating emulsion formation from dispersed particles in the mixed phase (pictured in the top frame). The samples tend to follow the left route on slow, shallow cooling and the right route on fast, deep cooling. Following slow, shallow cooling droplets of the minority phase nucleate and are stabilized by the colloids. Following fast, deep cooling extended liquid domains form as a result of spinodal decomposition. The interfaces, in both cases, are stabilized by a semisolid multilayer of particles.

smoother arrangement of colloids on the interface. The structure is bicontinuous: there are connecting pathways of both fluids across both long and short dimensions of the cell. This requires the presence of freestanding fluid necks within the slab, and at least two of these are visible in Figure 6a. Similar to some of the other morphologies we have created, these necks show clear departures from the condition of constant mean curvature required for static mechanical equilibrium of a fluid−fluid interface, Figure 6b. On the macroscale we are observing solid-like properties of

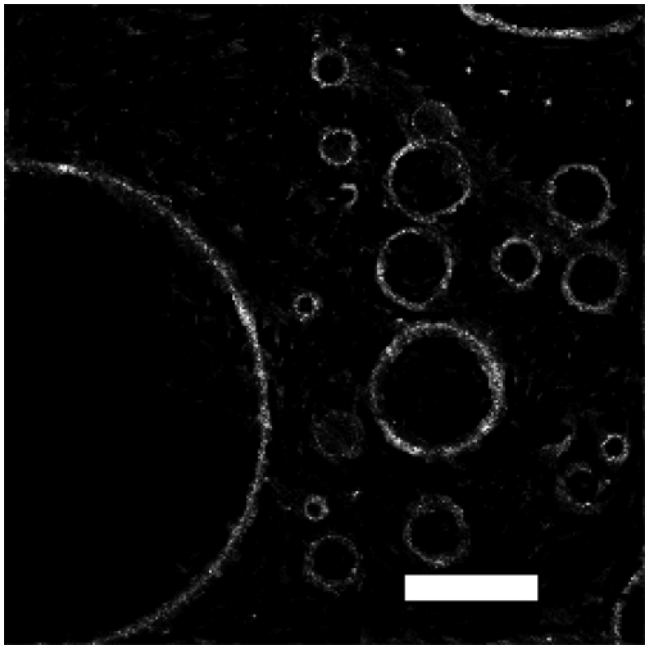

Figure 4. Confocal microscopy image of the droplets formed when an ethanol−dodecane mixture containing dispersed particles is cooled from 25 to 0 °C at 30 °C/min. The samples contain 43:57 ethanol: dodecane by volume, and the interfaces are stabilized by 1% volume fraction of silica particles (silanized with 10^{-1} M DCDMS). The scale bar is 100 μm, and the image was recorded with the sample at 0 °C.

the interface; we expect local fluidity will be maintained in the interstices. Similar particle-coated cylinders have been created by direct manipulation of air bubbles[11,12] and liquid jets.[13]

It remains unclear why liquid nitrogen cooling should be one of the successful routes toward creating these novel structures. It is evident from Figure 2 that this is not the fastest way of cooling (quite the reverse). It is, however, the deepest quench that we have explored. Liquid nitrogen is not essential. Convoluted structures have also been created using dry ice (e.g., Figure 5). One advantage of cooling with liquid nitrogen is that the interfaces move more slowly as a result of a slower quench. It is possible that the inertia or viscous drag associated with the silica particles is sufficiently high that they are not swept up by the passing interface at faster cooling rates (by analogy with ref 33). This is especially likely to happen at a very early stage during phase separation when the interfacial tension is low. An alternative advantage of using liquid nitrogen is that cooling the walls of the sample holder less quickly suppresses Tanakas' tube wetting scenario.[19] If the walls of the sample holder were wetted in this way the particle-laden structure would be solely composed of tubes running from one side of the sample to the other. Many of the dry ice cooled samples are characterized by vertical domains of the more hydrophilic phase (which will wet the capillary surface) with a circular cross-section.

Figure 7 shows structures created in a sample holder of double thickness (0.4 mm). This sample is comprised of an ethanol−dodecane mixture of composition 43:57 by volume. The white interfaces are silica particles (2% volume fraction) silanized with 10^{-1} M DCDMS. The sample was cooled by quenching from 28 °C for 30 s in liquid nitrogen and then for 5 min in an ice bath. It is evident that the structure is changing with depth into the sample. The morphology close to the sample surface appears to be bicontinuous. The structure closer to the center of the sample

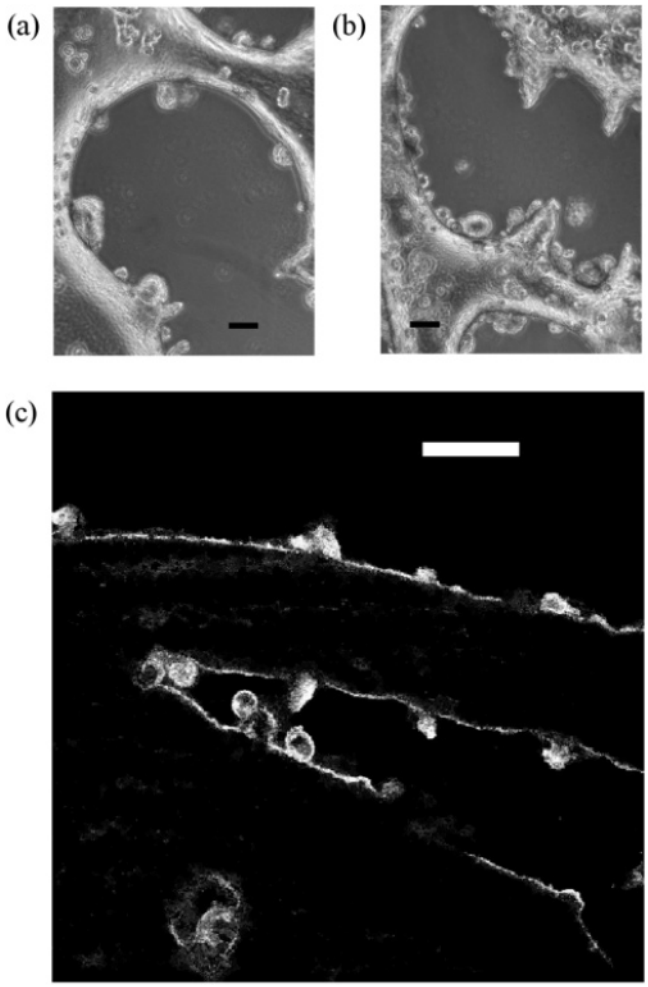

Figure 5. Phase-contrast (a and b) and reflection confocal (c) microscopy images of hexane domains in methanol. These samples were prepared in an incubator at 40 °C and cooled in a dry ice bath for 5 min. The composition is 38.7:61.3 alcohol:oil by volume, and the interface is stabilized by 1.3% volume fraction of particles (silanized with 10^{-2} M DCDMS). Frozen-in pinch off relics can clearly be seen in a and b. The scale bars are 100 μm; all images were recorded at room temperature.

reverts toward a colloid-stabilized droplet emulsion. We assume that this means it is taking too long to remove the heat from the center of the sample. The inset to Figure 2 shows the cooling rate for this size of sample holder relative to the 0.2 mm thick holders used for all other samples. The cooling rate at the center of the sample is substantially slower than that for cooling in an ice bath. Cooling too slowly results in nucleation and formation of a colloid-stabilized droplet emulsion. Results using different cryogens and different thicknesses of sample holder suggest that there is an optimal range of cooling rates for which formation of extended structures is possible.

3.2. Behavior of Droplets on Warming. We next describe the behavior of dodecane-rich droplets, Figure 4, on warming. The colloids (silanized with 10^{-1} M DCDMS) exhibit partial wettability with ethanol−dodecane phases, and so a deep energy minimum exists which keeps them at the interface, as described in section 1. The energy minimum results from the interfacial tension between the two liquids. On warming the emulsion toward the phase boundary two important changes will take place. First, as the emulsion moves toward miscibility, the composition of the two phases changes. This leads to a change in volume of the internal and external phases. This effect is shown schematically in Figure 8, where the variation in the volume fraction of the

(33) West, J. L.; Glushchenko, A.; Liao, G.; Reznikov, Y.; Andrienko, D.; Allen, M. P. *Phys. Rev. E* **2002**, *66*, 012702.

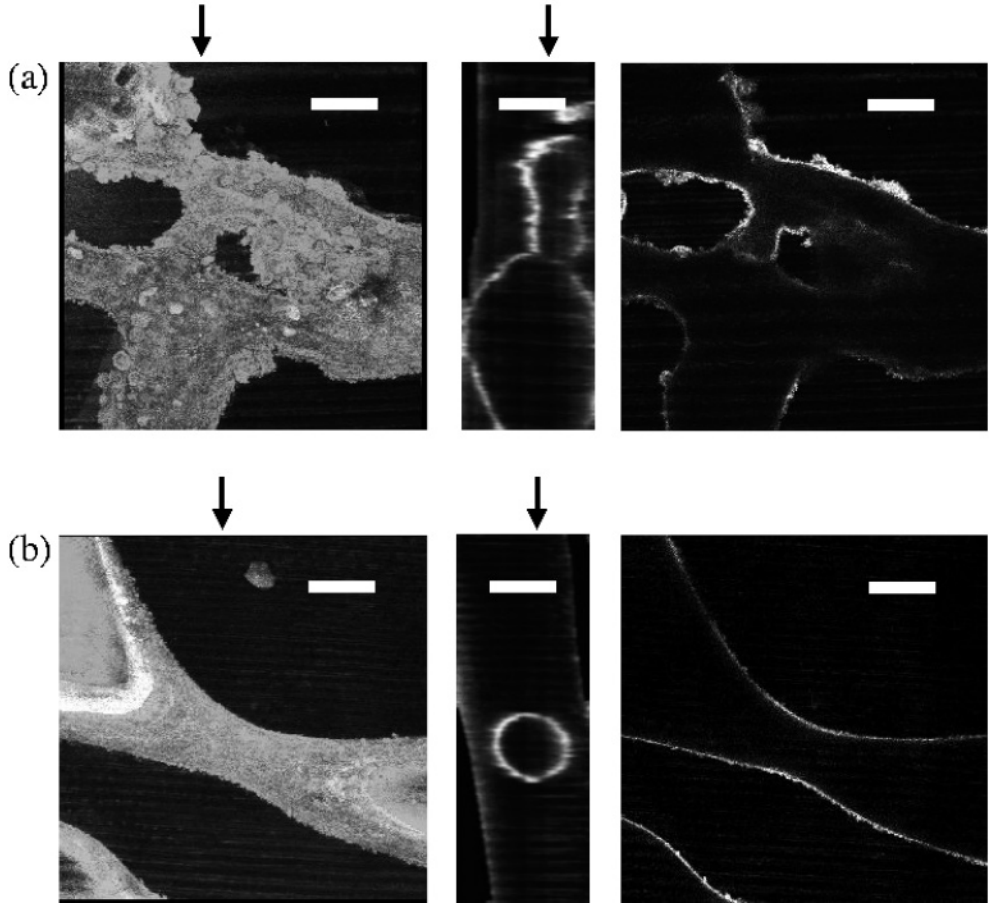

Figure 6. (Left) Rendered confocal images of 3D structures viewed from above; (center) vertical slices corresponding to the position of the arrow on the left; (right) horizontal slice through the confocal stack on left (corresponding to the position of the arrow in the center). (a) Arrested bicontinuous structure. (b) An isolated fluid neck, ending at contact lines with the glass plates confining the sample, stabilized by a colloidal multilayer. The liquid compositions and particle surface chemistry are the same as those for the samples in Figure 5. Here there are 2% volume fraction of particles. There are small differences in the quenching procedure between a and b as described in the text. All images were recorded at room temperature. Scale bars = 100 μm.

internal phase is sketched for the case of a parabolic binodal. Close to the phase boundary the decrease in volume is catastrophically rapid. Second, as the phase boundary is approached the interfacial tension will fall (albeit by a modest amount far from the critical point). This will decrease the energy barrier holding the particles to the interface. Taken together these changes suggest that the emulsion droplets will want to shrink as the protective barrier is becoming soft.

On warming well beyond the phase boundary the emulsion is ultimately destroyed. This obvious outcome belies more complex behavior. Two contrasting responses, indicative of semisolid surfaces, can be observed (Figure 9) and have previously been reported by us in a brief account.[21] The sample is being warmed at 2 °C/min. The first observation was that some droplets crumple on warming. It is likely that the integrity of the interface is lost and the internal volume falls dramatically as the phase composition attempts to adjust. A structure with a high bending modulus will tend to maintain its smoothly curved surfaces as it deflates. The elastic properties of the particle-laden interfaces are evidently dominated by the cost of stretching the interface. The second observation is droplets shattering. Sharp cracks can be seen in the droplet surface as the emulsion is warmed beyond the phase boundary. This behavior is likely to be associated with droplets for which there is very limited diffusion between the internal and external fluids. Presumably the interfaces are maintaining their integrity well beyond the phase boundary. The difference between internal and external compositions, compared to equilibrium, eventually results in catastrophic failure.

The behavior changes when the droplets are in close contact. Example observations are shown in Figure 10 for an ethanol−dodecane sample of critical composition. The interfaces (white) are stabilized by 2% volume fraction of silica colloids (silanized as described). The sample is being warmed at 30 °C/min (i.e., faster than the sample shown in Figure 9). The previously stable droplets become much more likely to coalesce as they are warmed. This suggests that the particle-laden interface is fluidized and in keeping with the expected diminishing of the interfacial tension. The particle-laden interface is able to support variations in the mean curvature for times long compared to the frame rate of these images. The droplets shown survive until well above the phase boundary. This hysteresis suggests that diffusion across the particle-laden interface is very slow. In the final frames of Figure 10 it is apparent that the particle-laden interfaces are becoming extremely broad. This is consistent with the colloids diffusing away as the interface ceases to exist. The extreme cases of crumpling and fracture (Figure 9) and coalescence (Figure 10) are the main evidence of the changing volumes of the dispersed and continuous phases (see Figure 8). No gradual decrease in the individual droplet size is observed (see Figure 10). This suggests that the phase diagram is modified by the interfacial colloids to support warming at constant volume fraction of the dispersed phase.

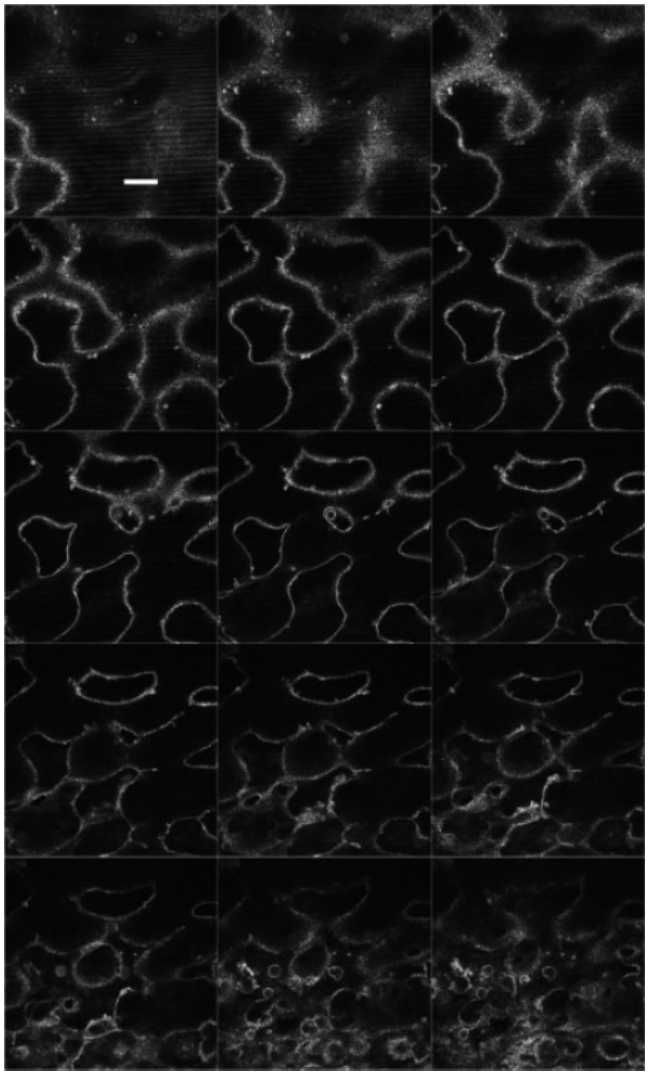

Figure 7. Confocal image recorded at 0 °C through an ethanol−dodecane structure (43:57 by volume) stabilized by 2% volume fraction of silica colloids (silanized using 10^{-1} M DCDMS). The sample was quenched from 28 °C by submerging for 30 s in liquid nitrogen and then 5 min in an ice bath. The scale bar is 100 μm. The stack extends a depth of 100 μm into a sample, which is 400 μm thick. The image sequence runs from top left to bottom right in steps of 6 μm.

One additional feature of these results is also important for our experiments: it can be seen in Figure 10 and elsewhere that the interfacial layer of particles is more than a monolayer thick. This phenomenon is likely to be due to residual attractions between the particles. As noted in section 2.1 the silica particles will attract one another within the more oily phase. The mechanism might be capillary wetting by polar impurities including, in this case, the alcohol. Multilayer formation is unavoidable in our system and has previously been studied using ellipsometry[24] at flat interfaces.

3.3. Behavior of Droplets during Thermal Cycling. In this section we describe the manipulation of preexisting droplets. We begin with droplets within the demixed region of the phase diagram. The emulsion is slowly warmed well into the mixed phase; as noted in section 3.2, there is considerable hysteresis. Droplets survive for tens of degrees above the phase boundary. Those droplets which are completely destroyed leave behind a population of dispersed particles within the mixed phase. Cooling the mixed state, comprised of some droplets and some dispersed particles, back into the demixed region yields emulsions with structures strongly dependent on the cooling rate. The situation is pictured in cartoon form in Figure 11 together with the outcomes of shallow and deep cooling.

Figure 12 shows particle-stabilized emulsion droplets before and after thermally cycling. All samples in section 3.3 have the same composition: they are hexane-in-methanol emulsions with liquid compositions 61.3:38.7 by volume. The interface is stabilized by 1% volume colloidal silica silanized using 10^{-2} M DCDMS. In this case the sample was warmed to 40 °C at 2 °C/min and held at that temperature for 5 min. It was quenched by submersion in an ice bath (see Figure 2). The before and after images show that, crudely, the typical droplet size has grown. More interestingly, the droplets now appear to be extensively distorted and a multiple emulsion has been formed. In keeping with Figure 10, it appears likely that the distorted droplets were formed by coalescence on warming (see cartoon Figure 11a). These droplets show clear departures from the condition of constant mean curvature required for static mechanical equilibrium of a fluid−fluid interface (at least on length scales large compared to the colloids). As described in section 1 this can occur if the surface is solid or has near zero interfacial tension. Since the surface imperfections are static in time, the former is the more likely interpretation.

Our measurements on warming droplets demonstrate that the internal phase has great difficulty reaching equilibrium with the continuous phase as the temperature is increased. In the case of warming this led to hysteresis (section 3.2). Something equivalent is also happening on cooling. Here the barrier preventing the dispersed and continuous phase reaching equilibrium is manifest in the abundance of multiple emulsion droplets. It appears that the fluid inside the pre-existing droplets has undergone its own independent phase separation. Since the internal phase is rich in hexane, on phase separation, the minority phase is rich in methanol. Hence, the multiple emulsion comprises large droplets with an internal phase rich in hexane which then contain smaller droplets rich in methanol. This scenario raises the question where do the particles come from to stabilize the internal emulsion? As described in section 3.2 we find that most of our samples exhibit interfaces that are more than a single particle layer thick. This may well be due to aggregation of particles in the oily phase (see also section 2.2). As methanol-rich regions nucleate from the oily phase we assume that they are stabilized by surplus particles from the interface.

Figure 13 shows particle-stabilized emulsion droplets before (Figure 13a) and after (Figure 13b−f) thermal cycling with two different quench depths. The images were taken with phase-contrast microscopy. The results following cooling in ice (Figure 13b,c) are consistent with those in Figure 12: droplets fuse and a multiple emulsion forms (Figure 13c). The last three images show the structure formed following precooling in liquid nitrogen before submerging in an ice bath (Figure 13d−f). As discussed above (section 2.2 and Figure 2), cooling in liquid nitrogen has a strong effect on the quench depth without speeding up the cooling rate. The images show an interconnected structure which appears to be largely composed of partially coalesced droplets. The structure is effectively two-dimensional since the sample is only a single domain (droplet) thick. Hence, the alcohol-filled regions are dark gray where they extend from one side of the sample to the other. Multiple emulsion formation is also evident. Figure 14 shows reflection confocal images of such structures. These samples are of the same composition; here they are pictured a day after they were created. It is clear that the droplets have fused, but the cause is not self-evident.

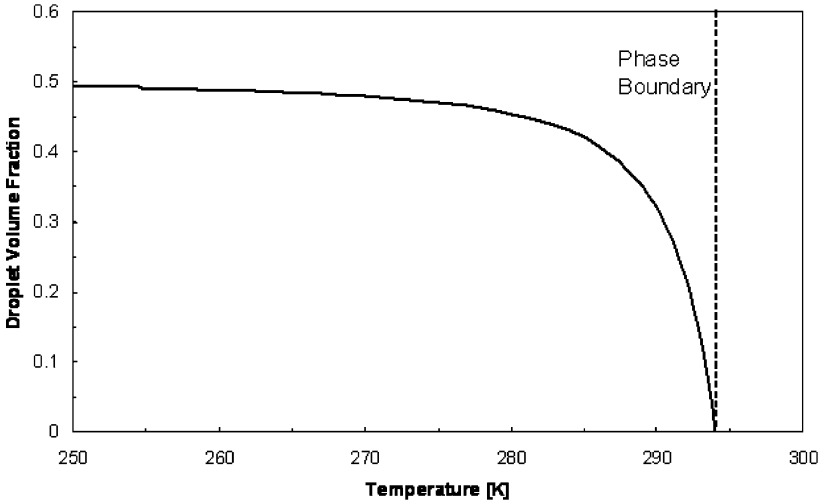

Figure 8. Sketch of the change in the internal volume of dispersed droplets as they are warmed from within the two-fluid phase toward the mixed phase. The illustration is for a system with a parabolic binodal and an off-critical composition. The internal volume falls precipitously close to the binodal.

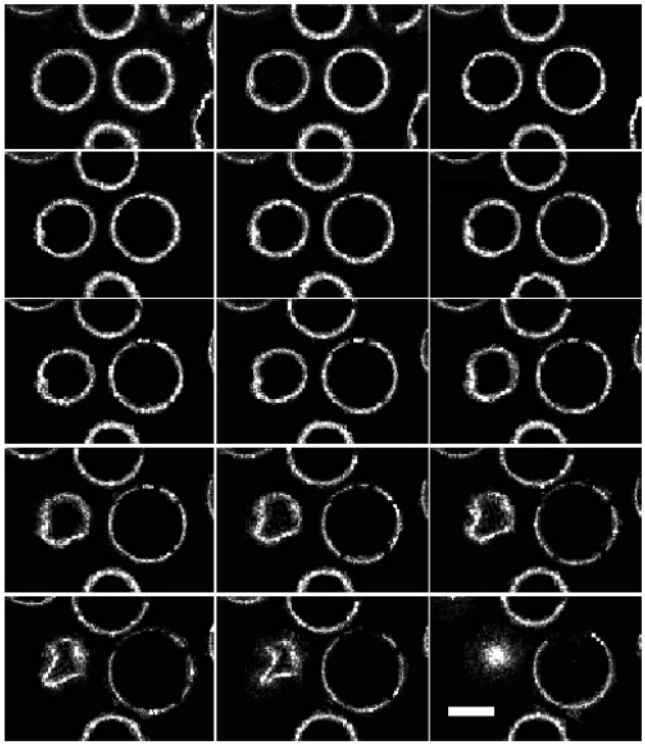

Figure 9. Confocal microscopy images of heptane-in-methanol droplets stabilized by 1% volume fraction of silica colloids (silanized using 10^{-2} M DCDMS). There is one frame every 60 s with each 2 °C higher in temperature than the previous one, starting at the top left. The sample is at the bulk demixing temperature in the fifth frame. As they are warmed some droplets are seen to deflate while others shatter. Particles can be seen to be diffusing away from the interfaces at high temperature. The images are at a depth of 40 μm, and the scale bar is 100 μm.

Formation of extended structures from fused droplets appears, at first sight, to be a natural extension of the behavior when pairs of droplets coalesce on warming. The droplets appear to be more highly distorted (including creases, see, e.g., Figures 13d,e and 14), while the size of the continuous fluid regions appears larger. These observations require explanation since the violent coalescence of droplets is not made more likely as a result of more extreme cooling. (A deeper quench implies that the system will be spending more of its time with high interfacial tension.) The surface texture of the droplets has also changed: it appears more rough. Also, unlike the case of cooling in ice, some regions have almost no resemblance to droplets (see, e.g., Figure 13f). To account for these observations we suggest that these novel emulsion states owe some of their character to heterogeneous nucleation. This kinetic pathway becomes increasingly favorable when the nucleation center is wet by the minority phase ($\theta_w = 0$ in eq 2). In our case the nucleation center is the existing droplets. These have interstitial regions where the minority phase is already exposed. This is a highly advantageous configuration for wetting. Wetting conditions will be particularly favorable in recessed interstices. Hence, heterogeneous nucleation will be more likely in the presence of droplets. To explain the morphology, we note that deep quenching results in some extended, convoluted domains seeded from existing droplets; droplets and extended domains are in contact. The particle-laden interface between a pre-existing droplet and the new domain that it has seeded will be unstable. Following heterogeneous nucleation the interface will have the oily phase on both sides, and so the energy barrier will no longer exist. Hence, following heterogeneous nucleation the seed droplets are likely to fuse with the newly formed domains (see cartoon Figure 11). The roughening of the interface may be the result of small regions of heterogeneous nucleation which was quickly arrested by a coverage of particles.

4. Conclusions

We studied colloid-stabilized emulsions in the context of binary liquids with a UCST. Within the demixed regime it is possible to create a colloid-stabilized droplet emulsion. Warming out of the demixed regime or quenching into it present opportunities to melt the emulsion surfaces or create emulsions with novel morphologies. The behavior of droplets at low temperature demonstrates that, on the macroscale, colloid-stabilized droplets have solid, or at least semisolid, surfaces. This is an essential prerequisite for creating some of the novel structures we observe. Our studies of warming and then cooling droplets resulted in formation of extended structures formed by partial coalescence. The morphology also depends on heterogeneous nucleation. A separate series of studies began with dispersed particles. Here we show that cooling leads to emulsion formation. The morphology of the emulsion depends on the speed and depth of cooling. The different structures formed are the result of differing demixing kinetics. Our studies demonstrate that it is possible to arrest the various microstructures formed during liquid−liquid

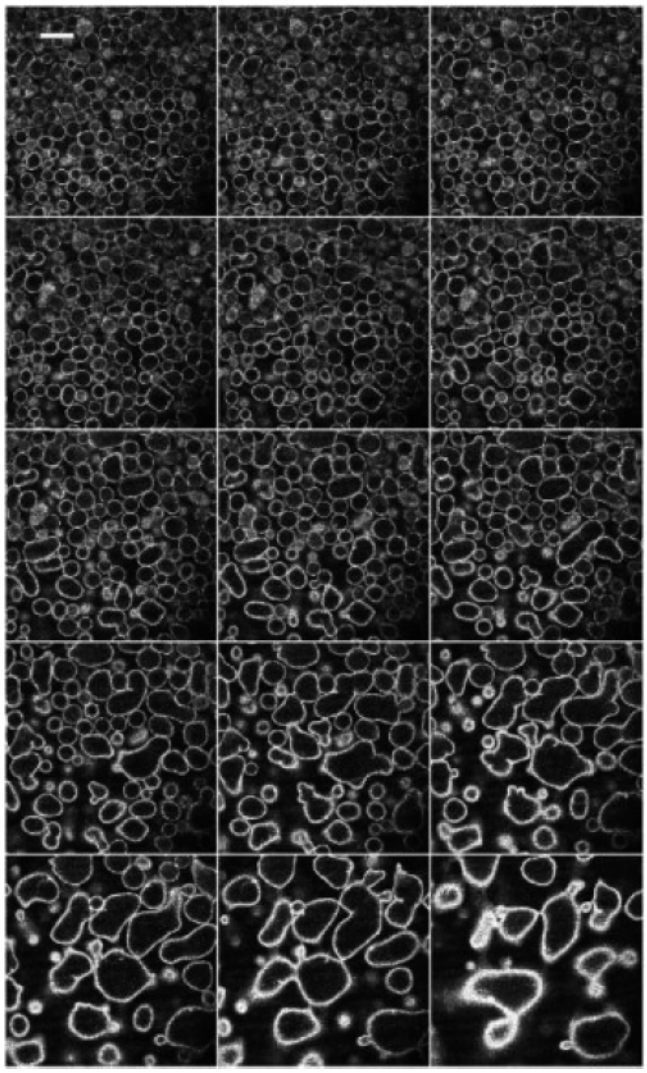

Figure 10. Confocal microscopy images of dodecane-rich droplets stabilized by silica particles as they are warmed beyond the binodal. The ethanol−dodecane sample has critical composition with 2% volume fraction of particles silanized with 10^{-1} M DCDMS. The sample was warmed from 0 to 41 °C at 30 °C/min, where all droplets had melted and particles had dispersed. The nominal temperature of the sample in the first frame (top left) is 9 °C and in the final frame (bottom right) 30 °C; each frame is 1.5 °C warmer than the last. The scale bar is 100 μm.

phase separation. Spinodal decomposition to form bicontinuous arrested states requires fast, deeper cooling: there is a limit to the thickness of samples that can currently be created by this route. A future goal is to create fully three-dimensional arrested structures, possibly via pressure-jump quenching or utilizing critical slowing down.

Our results on the quenching of dispersed colloids in phase-separating liquids can be illuminated by comparison with computer simulations of similar processes. Much of the research in this area has been reviewed by Balazs.[34] The two subsequent studies of greatest interest here are those by González-Segredo and Coveney[35] and by Stratford et al.[36]

The former study addresses the effect of amphiphilic surfactants on phase separation, while the latter concerns dispersed neutrally wetting colloids. Both use lattice Boltzmann methods well tested

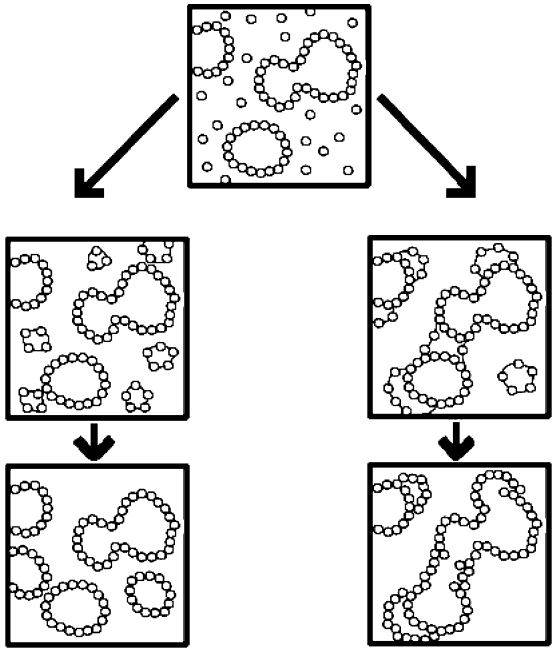

Figure 11. Cartoon illustrating emulsion formation in thermally cycled samples. The top frame shows a sample warmed into the mixed phase containing some coalesced droplets and some dispersed particles. The samples tend to follow the left route on shallow cooling and the right route on deep cooling. Following shallow cooling the sample is populated by the distorted droplets that survived being warmed to high temperature and also some new droplets that nucleated on cooling. Following deep cooling extended liquid domains form made up from pre-existing droplets. We suggest that heterogeneous nucleation plays an important role in creating the extended structures. This cartoon neglects formation of multiple emulsions.

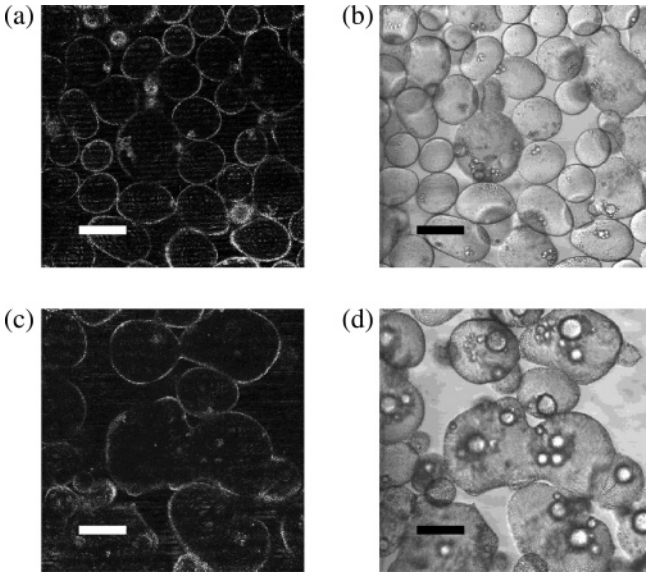

Figure 12. (a) Confocal and (b) bright-field microscopy images of a hexane-in-methanol emulsion (composition 61.3:38.7 by volume) stabilized by 1% volume fraction of silica colloids (silanized using 10^{-2} M DCDMS). Confocal images show the interface, while bright-field images show the contents of the droplets. (c) Confocal and (d) bright-field microscopy images of the same emulsion after it has been reheated and then quenched to 0 °C. These images were all captured at room temperature, and the scale bars are 100 μm.

on phase-separating fluids with no additives[37,38] In both cases the role of the surface active ingredient is to arrest phase

(34) Balazs, A. C. *Curr. Opin. Colloid Interface Sci.* **2000**, *4*, 443.
(35) González-Segredo, N.; Coveney, P. V. *Phys. Rev. E* **2004**, *69*, 061501.
(36) Stratford, K.; Adhikari, R.; Pagonabarraga, I.; Desplat, J.-C.; Cates, M. E. *Science* **2005**, *309*, 2198.
(37) González-Segredo, N.; Nekovee, M.; Coveney, P. V. *Phys. Rev. E* **2003**, *67*, 046304.

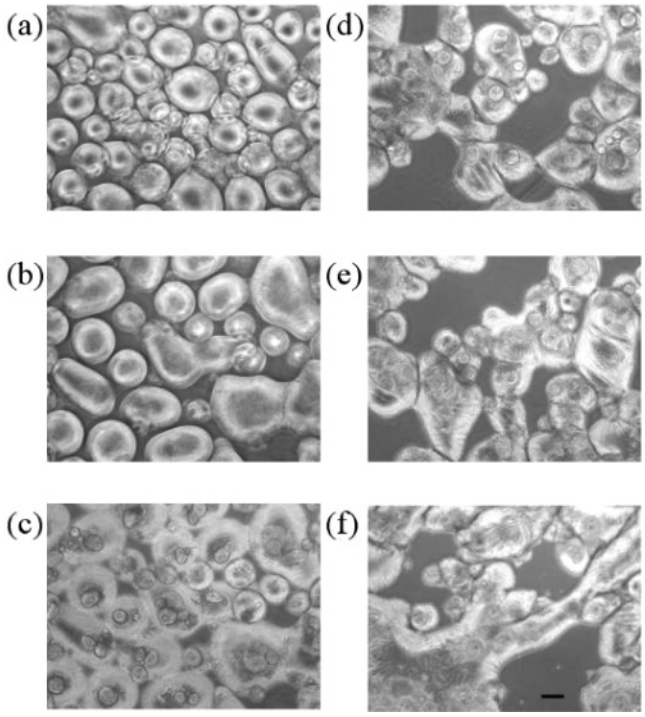

Figure 13. Phase-contrast microscopy images (scale bar = 100 μm.) of hexane droplets in methanol (a) before quenching, (b) after quenching in an ice bath, (c) as in b but focused deeper into the sample, and (d−f) after precooling for 4 s in liquid nitrogen and then cooling in an ice bath. The composition of all these samples is 38.7:61.3 alcohol:oil by volume, and the interface is stabilized by 1% volume fraction of particles (silanized with 10^{-2} M DCDMS).

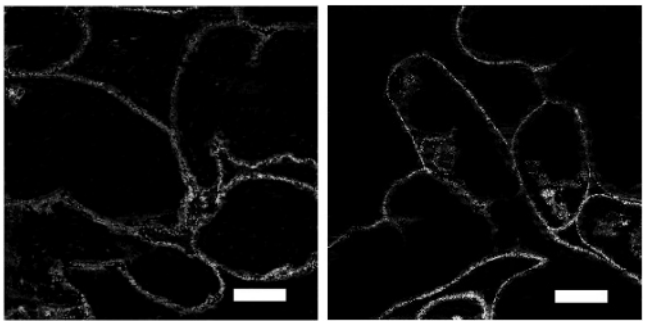

Figure 14. Confocal microscopy images of an arrested structure created from thermally cycled droplets (sample composition 38.7: 61.3 methanol:hexane). The internal phase is rich in hexane with 1% volume fraction of particles (silanized with 10^{-2} M DCDMS). The samples, both prepared identically, were warmed to 40 °C at 2 °C/ min and held at that temperature for 5 min. They were then precooled for 5 s in liquid nitrogen before being submerged in an ice bath. These samples were at room temperature for 24 h prior to imaging. The scale bars are 100 μm.

separation, but the mechanisms leading to arrest are very different in the two cases. During phase separation amphiphiles are swept up onto the newly created interface.[35] In this case the interfacial tension immediately begins to fall. This means that the force driving the coarsening of domains begins to diminish and phase separation slows. When the concentration of amphiphiles on the interface becomes sufficient for the interfacial tension to be near zero the phase separation arrests. The arrested state is dynamic; there is a population of amphiphiles in fluid domains, and the interfacial structure strongly fluctuates. This is as expected for

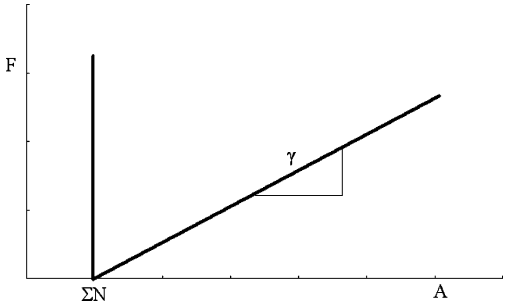

Figure 15. Variation in free energy, F, with the interfacial area, A. Here, Σ is the area per particle, while N is the number of particles. The macroscopic interfacial tension, γ, is not a helpful concept for colloid-stabilized emulsions.

an equilibrium microemulsion.[39] The second series of simulations show that neutrally wetting colloids are also swept up onto the newly created interface during phase separation.[36] Here there is little or no change in the interfacial tension and colloids (see the Appendix), once trapped on the interface, do not escape. Arrest occurs when there is a high density of colloids on the interface. The repulsion between neighboring colloids (irreversibly trapped) is sufficient to prevent a further reduction in the interfacial area. The colloid-stabilized structures can be anticipated to have solid-like properties as a result of the jammed rigid interface.

The simulations of dispersed colloids are more relevant to the experimental results presented here. We observed the arrest of phase separation due to an interfacial layer of colloids. Hence, some aspects of the simulations in ref 36 are confirmed by our results. However, there are substantial differences between our results and the computational studies. First, our samples are thin in one direction (with sample size comparable to the domain length scale) and hence quasi-two-dimensional. Second, our interfaces are covered by more than a monolayer of particles. These two differences are associated with the need to cool the samples rapidly and with the residual attractive interactions between the particles. Nonetheless, our results presented in section 3.1 are broadly consistent with the lattice Boltzmann results.[36] The associated mechanism of arrest, explored in ref 36, suggests that our structures will be mechanically rigid and support counter flowing liquids. Future studies are planned to explore these predictions. Additionally, the simulations of arrest due to amphiphiles demonstrate that formation of ordered mesophases during phase separation is not chemically specific but can occur in simple model systems.[35] It is of great interest to see if ordered mesophases can be formed between binary liquids stabilized by an interfacial layer of particles.

Acknowledgment. We are very grateful to D. Roux for illuminating discussions. Funding in Edinburgh was provided by EPSRC Grant GR/S10377/01.

Appendix: Interfacial Tension

Note that an important distinction exists between the macroscopic interfacial tension of a colloid coated interface and one coated with soluble amphiphiles. In the latter case, the interfacial tension is controlled by the surfactant activity, which (since the bulk phases act as a reservoir) is independent of interfacial area. If the interface expands or contracts, amphiphiles are adsorbed or desorbed to maintain constant tension. Due to the high barriers involved, for a colloid-coated surface, small changes in area are not balanced by changes in the interfacial colloid population.

(38) Kendon, V. M.; Cates, M. E.; Pagonabarraga, I.; Desplat, J.-C.; Bladdon, P. *J. Fluid Mech.* **2001**, *440*, 147.

(39) Safran, S. A. *Statistical Thermodynamics of Surfaces, Interfaces, and Membranes*; Addison-Wesley: Menlo Park, 1994.

Hence, even if the initial interfacial film is at a minimum of free energy F for the given colloid population N (which technically would be a state of zero tension for the film, $\partial F/\partial A|_N = 0$), any noninfinitesimal increase of area creates unprotected interface with a cost governed by the bare tension, γ, between the two fluids. A *decrease* in the macroscopic film area also requires colloids to leave the plane of the film, giving an energy *increase*; such a film cannot in fact be described by surface tension but instead requires an interfacial elasticity model. This is closely analogous to the case of insoluble lipid films which are, paradoxically, often described as being simultaneously (a) in a state of zero surface tension and (b) unable to change in area.[39] In the lipid case, this is resolved by noting that $F(A,N)$ has a quadratic minimum of very high curvature at some fixed area per lipid $A/N = \Sigma$; hence, $\partial F/\partial A|_{N=A/\Sigma}$ is indeed zero, but dilational elasticity prohibits changes in area. For a flat jammed monolayer film of hard-sphere colloids at zero temperature (no Brownian motion) the resulting $F(A,N)$ is not quadratic but V-shaped (Figure 15), F with $F \rightarrow \infty$ (sphere overlap) for $A < \Sigma N$ and $F = \gamma(A - N\pi r^2)$ for $A > \Sigma N$. Here, Σ is the macroscopic area per colloid in the close-packed jammed layer (whether amorphous or crystalline). Allowing for Brownian motion, the cusp in $F(A,N)$ is smoothed out to create a quadratic minimum reminiscent of that seen for lipids.

In view of the above it is not surprising to find in the literature[8] contradictory data concerning the magnitude of the macroscopic interfacial tension of jammed colloidal films. The concept of macroscopic tension $\partial F/\partial A|_N$ is not helpful since in the proximity of the jammed state with $A = \Sigma N$, $\partial F/\partial A|_N$ switches from $-\infty$ via zero to $+\gamma$ within an infinitesimal range of area variation (Figure 15).

LA063707T